Universal Journal of Carbon Research
https://ojs.wiserpub.com/index.php/UJCR/

Research Article

Strength Characteristics of Carbon Fiber Reinforced Plastic in Shear and Cyclic Extension-Compression after 7 Years of Climate Exposure

Petrov M.G.[1*], Startsev O.V.[2], Lebedev M.P.[2], Kopyrin M.M.[2], Salnikov V.G.[3]

[1]Siberian Aeronautical Research Institute named after S.A. Chaplygin, 630051 Novosibirsk, Russia
[2]Yakut Scientific Center, Siberian Branch of Russian Academy of Sciences, 677980 Yakutsk, Russia
[3]Branch of Natural-Technical Systems Institute, 354000 Sochi, Russia
E-mail: mark-stein@list.ru

Received: 19 December 2023; **Revised:** 26 February 2024; **Accepted:** 28 February 2024

Abstract: The results of studies of carbon fiber reinforced plastic (CFRP) for aviation purposes based on the Cycom 977-2 epoxy binder and Tenax® IMS carbon fibers after 7 years of exposure under a canopy and on an open atmospheric stand in the warm humid climate of Sochi are presented. The influence of climatic aging is determined by the change in strength parameters during interlaminar shear and cyclic tension – compression. After exposure under a canopy, the strength characteristics during interlaminar shear and cyclic tension–compression increase by 7–13 %. If the plate is under the direct influence of solar radiation, then the strength characteristics of the material are slightly reduced, but remain at the level of the original values. The kinetic concept of fracture was used to interpret the results. The thermal activation analysis showed that the characteristics of the inelasticity of the plate specimens, both in terms of the relaxation and hysteresis parts of energy absorption, correspond to their strength characteristics.

***Keywords*:** CFRP; strength, interlaminar shear; tension–compression; fracture activation energy; thermal activation analysis

1. Introduction

CFRP based on thermosetting matrices have the highest climatic resistance compared to fiberglass (FG), organ plastics (OP) and other polymer composite materials (PCM) [1, 2]. Nevertheless, these materials also degrade their mechanical properties when exposed in open climatic conditions [3]. For example, Table 1 shows the values of the relative retention coefficients of $k_P = P/P_0$, where are the strength limits and elastic modulus under tension (σ_t, E_t), compression (σ_c, E_c), bending (σ_b, E_b), interlaminar shear (τ, G) and P_0 are the initial values of the corresponding indicators.

There are examples showing that after 5 years of staying in open climatic conditions, the CFRP decreases the P values by more than 20 % [10, 11]. Therefore, measuring the k_P values of these materials after prolonged climatic exposure is relevant for practice and elucidation of aging mechanisms [12].

Among the PCM, the study of climatic aging of aviation equipment is of particular interest [3]. For example, Boeing 787 and Airbus A380 designs use materials based on Cycom 977-2 epoxy binder and IM7, T800, HTS40 carbon fibers [13, 14]. By adjusting the reinforcement scheme [13] and pressing modes [14], it is possible to

DOI: https://doi.org/10.37256/2120244131

achieve the levels of indicators necessary for the construction of loaded structural elements. In the works [15, 16], it was reported on the levels of moisture saturation of CFRP based on Cycom 977-2, including during 6 years of exposure of this material in a warm humid climate [16].

The review article [17] substantiates the need to take into account internal stresses when predicting mechanical parameters in polymer-composite materials (PCMs) subject to climatic aging. The patterns of formation and development of micro-cracks under cyclic mechanical loads are considered. It is shown that similar micro-cracks are formed in PCMs due to the action of internal stresses during thermal and thermal-moisture cycling, during the transformation of absorbed water into ice. The nature of micro-cracking depends on the properties and morphology of polymer matrices and fibers, the number of cycles, the type of stacking, temperature difference, bond strength, the ratio of strength and deformation at the micro- and macro-levels, and other factors. The processes of thermal oxidation and photo-oxidation activate microc-racking of polymer matrices in PCMs, proving the need for a profound inquiry into the density of micro-cracks in open climatic conditions.

Table 1. Changes in the mechanical properties of carbon fiber plastics after exposure in open climatic conditions

Марка углепластика	Test conditions		Values of the P, МПа				Refe-rence
	Site	Time, years	P	P_0^*	P_t^{**}	$k_P = P_t/P_0$	
T-300/E-788	Alaska	10	σ_c	828	811	0,98	[1]
			τ	78,7	74,8	0,95	
KMU-1	Batumi	11	σ_b	800	720	0,90	[4]
			E_b	165000	102000	0,62	
KMU -1u	Batumi	10	σ_b	480	494	1,03	[5]
			E_b	88000	92500	1,05	
			σ_c	260	256	0,98	
T300/2544	San Diego	10	σ_c	1028	883	0,86	[6]
	Wellington		τ	80,6	73,3	0,91	
T-300/5209	San Diego		E_b	104000	98500	0,95	
Epoxy laminate $[0]_8$	Choshi,	13	σ_b	2174	2126	0,98	[7]
Epoxy laminate $[90]_8$				104	89,4	0,86	
AS4/3501-6	Australia	10	τ	72,9	75,2	1,03	[8]
KMU -3ln [0,90]	Batumi	5	σ_b	950	900	0,95	[2]
			E_b	112000	103000	0,92	
KMU -4l [0,90]	Batumi	5	σ_b	500	540	1,08	
VKU-38	Sochi	5	σ_t	350	365	1,04	[9]
			σ_c	234	245	1,05	
	Moscow		σ_t	350	320	0,91	
			σ_c	234	215	0,92	
VKU -38ZhN	Sochi	5	σ_t	1300	1070	0,82	
			σ_c	670	550	0,82	
	Moscow		σ_t	1300	1160	0,89	
			σ_c	670	530	0,79	
VKU -38TR	Sochi	5	σ_t	740	730	0,99	
			σ_b	670	740	1,10	
	Moscow		σ_t	740	740	1,0	
			σ_b	670	740	1,10	
VKU -45Zh	Sochi	5	σ_c	660	500	0,76	[10]
	Moscow				500	0,76	
VKU -45/3692	Sochi			610	628	1,03	
	Moscow				572	0,94	
VKU -51	Gelendzhik	5	σ_t	729	786	1,08	[11]
			E_t	61	66	1,08	
			σ_b	663	632	0,95	
			E_b	63	48	0,76	

* in its original state, ** after exposure

The service life of CFRP used in an aircraft intended for operation under Arctic extreme conditions was studied [18] by longitudinal bend testing in which monotonic loading at various rates of displacement of the mobile gripper of a testing machine was combined with cyclic loading of specimens with increasing displacement range. The force dependences of the activation energy of failure and the dependences between the failure rate, deformation rate, and service life were characterized. Exposure of CFRP to subfreezing temperatures was shown to hardly affect the service life. However, periodic transitions through the crystallization temperature of water accumulated in the composite significantly impair its strength performance and safe service life.

Asasaari et al. [19] revealed a decrease in the mechanical parameters of PCM during moisture saturation. Exposure of CFRP in open climatic conditions according to the data of [20, 21] showed that as a result of exposure to temperature, freezing-thawing processes, marine chlorides in the air, aging occurs, accompanied by a change

in mechanical properties. According to Shi et al. [22] CFRP aging grows under the influence of the ultraviolet component of solar radiation.

The purpose of our work is to determine the effect of long-term climatic conditions on the mechanical properties of the same CFRP. It is expected to identify differences in the strength characteristics of CFRP after prolonged exposure on an open stand and under a canopy in a warm, humid marine climate.

2. The experimental part

For the research, an CFRP was used, the components of which are an epoxy binder of the Cycom 977-2 type, cured at a temperature of 177 °C, and reinforcement — carbon fiber of the Tenax ® IMS brand with a thread diameter of 5 microns. The panels of the CFRP were manufactured using prepreg technology followed by autoclave molding. Panels with multilayer stacking [−45/0/+45/0/0/90/0/0/+45/0/−45] were used for the study. The choice of the installation method is determined by the design requirements to ensure the rigidity and strength of the panels in the reinforcement plane. Plates measuring 150 mm × 100 mm × 6.5 mm were cut out of the panels. Before the start of the tests, the plates were kept in an air thermostat at 60 °C until the mass was stabilized, after which they were tested for 7 years for the effects of the warm humid climate of Sochi.

Plate 1 was stored in the laboratory. It can be considered as a plate corresponding to the initial state. Plate 2 was under a canopy and was exposed to temperature and natural humidity. According to [16], 0.3 ± 0.05% of moisture accumulated in it. The same amount of moisture was contained in plates 1 and 3.

Plate 3 was exhibited on an open stand at an angle of 45° to the horizon. Due to daily and seasonal fluctuations in air temperature under the influence of solar radiation, the plate was heated to 25 °C and conditions were formed for more intensive moisture transfer (sorption at high humidity and rains and desorption during heating) and the formation of micro-cracks due to different values of the coefficients of linear thermal expansion of the polymer matrix and reinforcing fibers [12]. Under the influence of the ultraviolet component of solar radiation, the destruction of the thin surface layer of plate 3 occurred, over 7 years of climatic tests, and its mass decreased by 0.5 ± 0.05% [16].

After the completion of climatic tests, the strength properties of the CFRP were studied by two methods: interlaminar shear and cyclic tension–compression.

For interlaminar shear tests, 12 specimens were cut from each plate with dimensions of 50 mm × 12 mm × 6.5 mm. The loading was carried out by moving the rod of the test machine with different rates in the range of their variation in each experiment, amounting to three orders of magnitude: from 0.1 to 0.0001 mm/s. This made it possible to conduct a thermal activation analysis of the failure process of specimens as a temporary thermodynamic process.

The tests were carried out according to GOST 32659-2014 for three-point bending, and the maximum values of tangential stresses are determined by the formula

$$\tau_{max} = 3F / 4S \quad (1)$$

where F is the load, S is the cross-sectional area of the specimen. The loads were carried out on a machine with an electric drive of a movable rod of the BiSS-10 kN brand (Bangalore integrated System Solutions, India). The view of the fracturing specimen mounted on the test machine is shown in Figure 1.

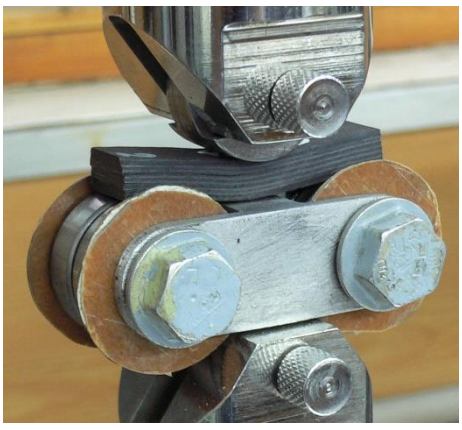

Figure 1. Process of specimen failure by interlaminar shear in test machine

For cyclic loads, three specimens of 150 mm × 28 mm × 6.5 mm with a radius of 40 mm in the middle part up to a transverse size of 10 mm were cut out (so-called corset specimen). The loading was carried out in a symmetrical harmonic cycle at a frequency of 0.5 Hz with an amplitude step of 10 MPa, four cycles at each amplitude value. In three repetitive cycles, excluding transient ones, and for each loading amplitude was determined the width of the inelasticity loop. Then, its amplitude dependence was constructed, according to which the amplitude of the appearance of plastic hysteresis was determined. The drawing of the test specimen and the loading program are shown in Figure 2. The tests were carried out on an electro-hydraulic machine BiSS-100 kN.

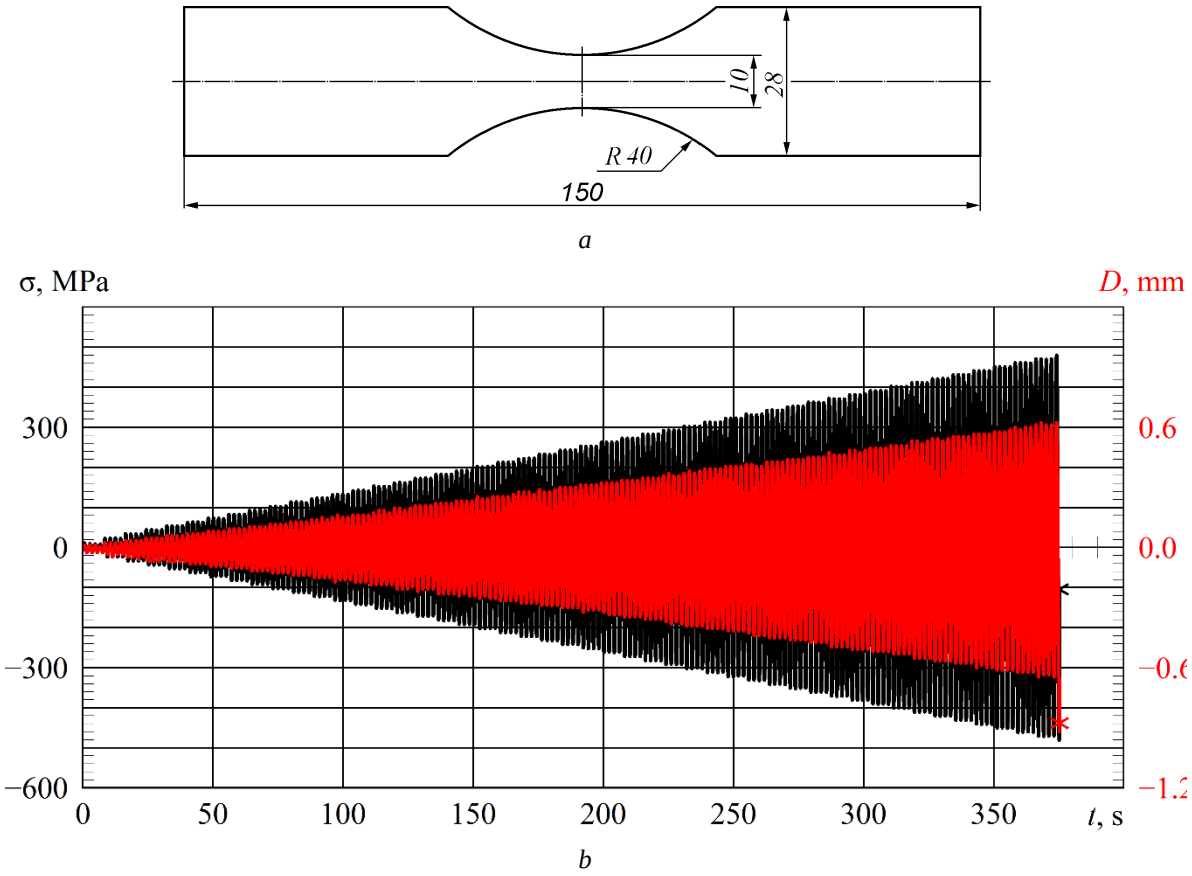

Figure 2. Specimen drawing (*a*) and loading program with a stepwise increase in amplitude of a specimen of plate 1 (*b*). The moments of final fracture of the specimen are noted. *D* is displacements along the length of the working part of the specimen

If the specimen did not failure in the first loading block at a maximum stress of 500 MPa, a second block was performed in which the specimen failed at a lower load. Some specimens were tested in one block, loading them to larger amplitude. The version of the loading program does not matter, since thermal activation analysis leads all experimental data to a single characteristic of the strength of the specimens.

3. Results of interlaminar shear tests

With three-point bending of the specimens of plate 1 at different loading rates, the dependences of the maximum tangential stresses on the loading time are obtained, shown in Figure 3. Similar dependences are also obtained for specimens cut from plates 2 and 3.

It turned out that the maximum tangential stresses during the failure of the specimens decrease in proportion to the logarithm of the loading time. Similar dependences were obtained in [23–25] for the strength parameters of carbon fiber plastics. The increase in strength indicators with an increase in the loading rate of the PCM is explained by the thermal fluctuation nature of the strength [26].

Therefore, based on the test results obtained for each plate, a thermal activation analysis was performed in accordance with the time trajectory of loading of each specimen. To do this, an equivalent failure time was calculated, which corresponds to the damage of the material to its residence time at maximum stresses τ_{max}, if they were kept constant during the experiment.

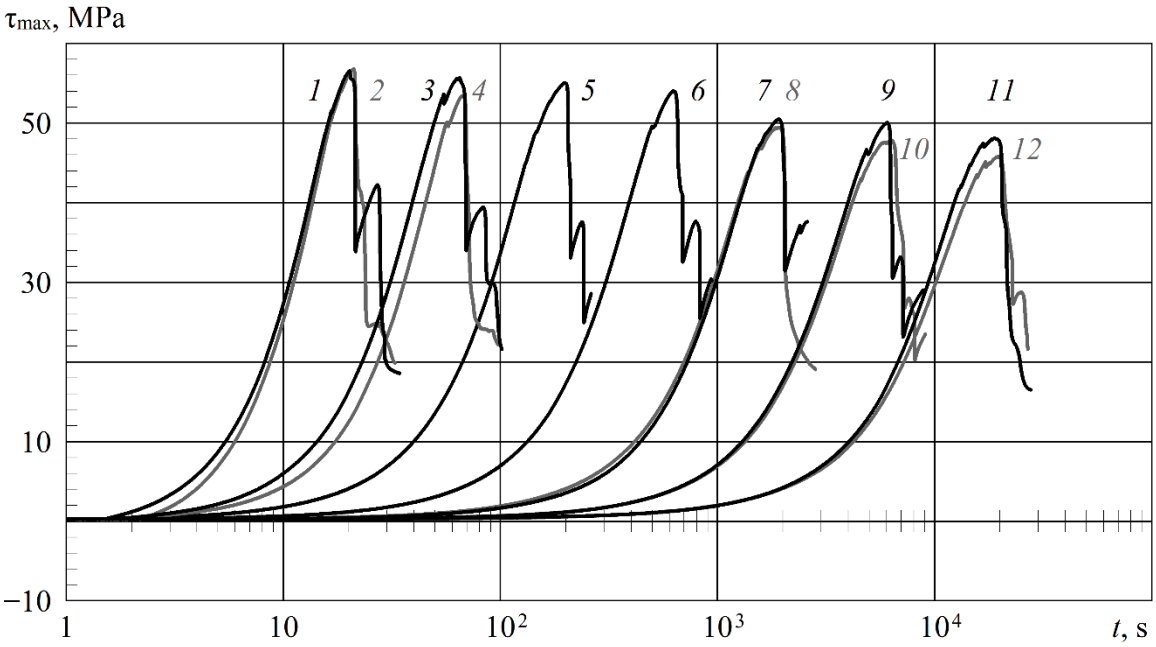

Figure 3. Dependence of the maximum values of shear stresses in the specimens of plate 1 on time during loading by displacement with rates (mm/s): 0,1 (*1*, *2*); 0,03 (*3*, *4*); 0,01 (*5*); 0,03 (*6*); 0,001 (*7*, *8*); 0,0001 (*9*, *10*); 0,0003 (*11*, *12*)

The equivalent failure time τ_{eq} is calculated based on the equality of damage according to the equation

$$\int_0^{t_*} \dot{\omega}\left(t, \tau_{\max}\right) \mathrm{d}\, t = \tau_{eq} \nu_0 \exp\left(-\frac{U_0 - \gamma \tau_{\max}}{RT}\right), \tag{2}$$

where $\dot{\omega} = \mathrm{d}\,\omega / \mathrm{d}\,t$ is the rate of failure, depending on time. It is a value, the inverse of durability, and is defined by the expression

$$\dot{\omega} = \nu_0 \exp\left(-\frac{U_0 - \gamma \tau_{\max}}{RT}\right). \tag{3}$$

Here t is time, t_* is the moment of time corresponding to the end of the failure process, U_0 is the initial fracture activation energy (FAE), γ is a structurally sensitive parameter, R is the universal gas constant, T is the absolute temperature.

The thermal activation analysis consists in obtaining the force dependences of the FAE in equation (3), which characterize the failure process from the point of view of thermodynamics. This expression is $U_0 - \gamma\tau_{\max}$ in (3). Parameter γ is structural sensitive coefficient corresponding to the overload of atomic bonds [26].

To do this, the $U(\tau_{\max})$ dependencies were built as a set of values

$$U_i(\tau_{\max}) = RT \ln(\tau_{eq} \nu_0), \tag{4}$$

obtained from (2) by multiplying the natural logarithm of the product by $\tau_{eq}\nu_0$ and RT, $\nu_0 = 10^{13}$ s^{-1} is the characteristic Debye frequency.

The dependences $U(\tau_{\max})$ (4) were calculated by the least squares method under the assumption of the constancy U_0, which does not depend on the structure of CFRP in the process of failure [26]. The integration in equation (2) is performed numerically in time steps, according to the frequency of digitization of data, assuming a linear stresses change at the time step.

For plate 1, the dependence of U on $\tau_{\max}$ is linear (Figure 4), from which the initial FAE is determined by extrapolating the values of $U_i(\tau_{\max})$ to $\tau_{\max} = 0$. The value of U_0 turned out to be 155.3 ±8 kJ/mol.

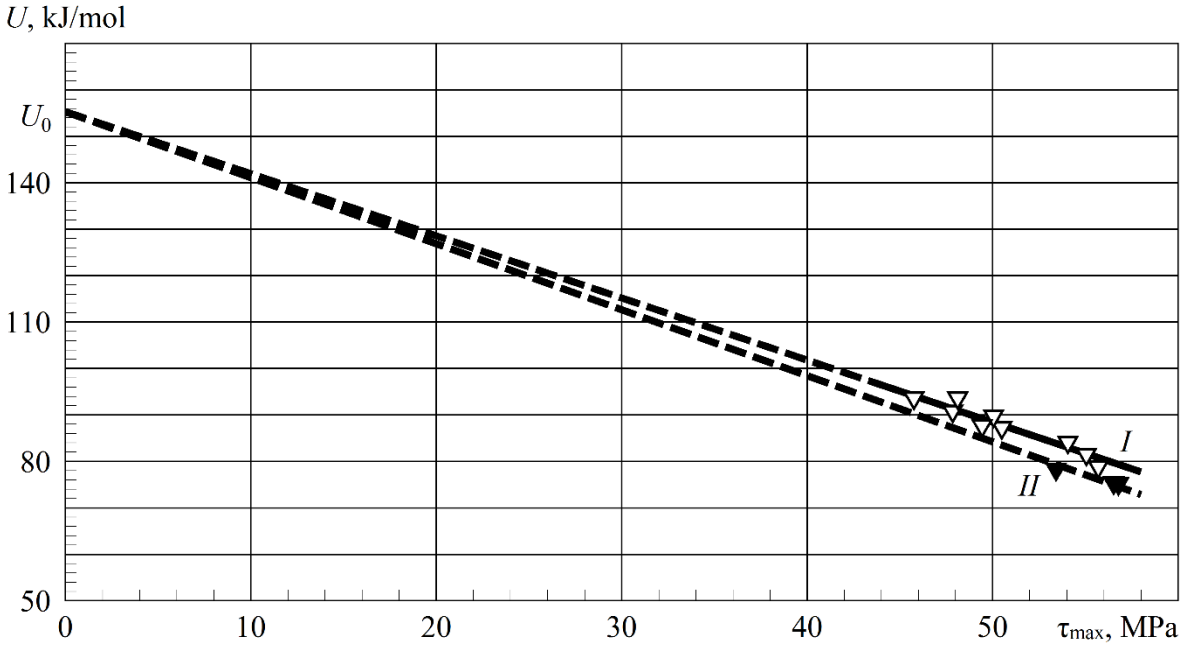

Figure 4. Force dependences of the FAE of plate 1 specimens during interlaminar shear with different displacement rates: *I* — minimum value γ for specimens 3, 5–12; *II* — increased value γ for specimens 1, 2, 4

Similar results were obtained for specimens from plates 2 and 3. Comparison of the results of interlaminar shear in various structural states of the binder was carried out according to the shear strength parameter

$$P_{sh} = \frac{\tau_{max}}{U_0 - U_i} = \frac{1}{\gamma}, \quad (5)$$

which does not depend on the loading rate and temperature, but characterizes only the state of the material structure by the value of the structurally sensitive parameter (activation volume) γ.

The results of the comparison are presented in the Table 2. After 7 years of exposure under a canopy, the τ_{max} and P_{sh} values of carbon fiber increase by 7–8 %. A possible reason for this increase is the processes of structural relaxation and before the curing of the binder, initiated by daily and seasonal fluctuations in temperature and relative humidity in open climatic conditions [16, 27, and 28]. Under the influence of solar radiation, the surface layer of plate 3 is destroyed. This causes an insignificant decrease in the τ_{max} index compared to the initial state, but the P_{sh} value remains higher than in plate 1 with a doubling of the scatter in the FAE for individual specimens.

Table 2. Properties of interlaminar shear properties of carbon fiber Cycom 977-2/Tenax after 7 years of climatic tests in a warm humid climate

Test conditions	τ_{max}, MPa	P_{sh}, MPa·mol/kJ
In the laboratory	51.9	0.73
An exhibition under a canopy	55.4	0.79
An exhibition on an open stand	50.9	0.77

4. The results of cyclic tension – compression tests

During the cyclic tension–compression tests, an accumulation of residual strains in the direction of tension was detected. This usually indicates insufficient fiber tension in the manufacture of specimens. In specimens where the fibers are well stretched, everything happens as it should be: the material is deformed in the direction in which the stresses act, leading to its fracture. Figure 5 shows the change in the rigidity *R* of the specimen from plate 2 and the accumulation of residual strains D_0 in it as the stress amplitude σ_a increases. The change in the rigidity of the specimens was calculated by the inclination of the loops of inelasticity, the accumulation of residual strains was determined by the displacement of the loops relative to the first loading cycle at σ = 0.

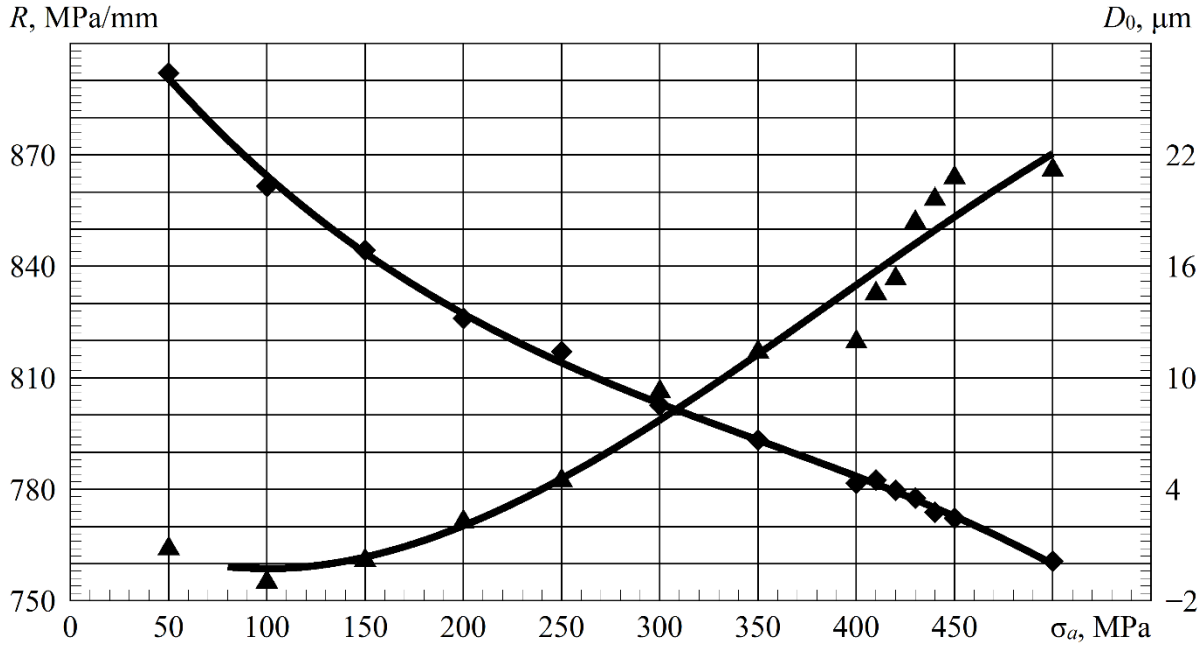

Figure 5. Reduction of rigidity and accumulation of residual strains of the specimen from plate 2 in the direction of tensile stresses when it is loaded with increasing stress amplitude up to 500 MPa

Figure 6 shows the shape of the inelasticity loops with an amplitude step of 50 MPa for the specimen from plate 1. It can be seen that the inelasticity loops up to fracture at σ_{max} = 458 MPa have almost the same shape both under tensile and compressive stresses.

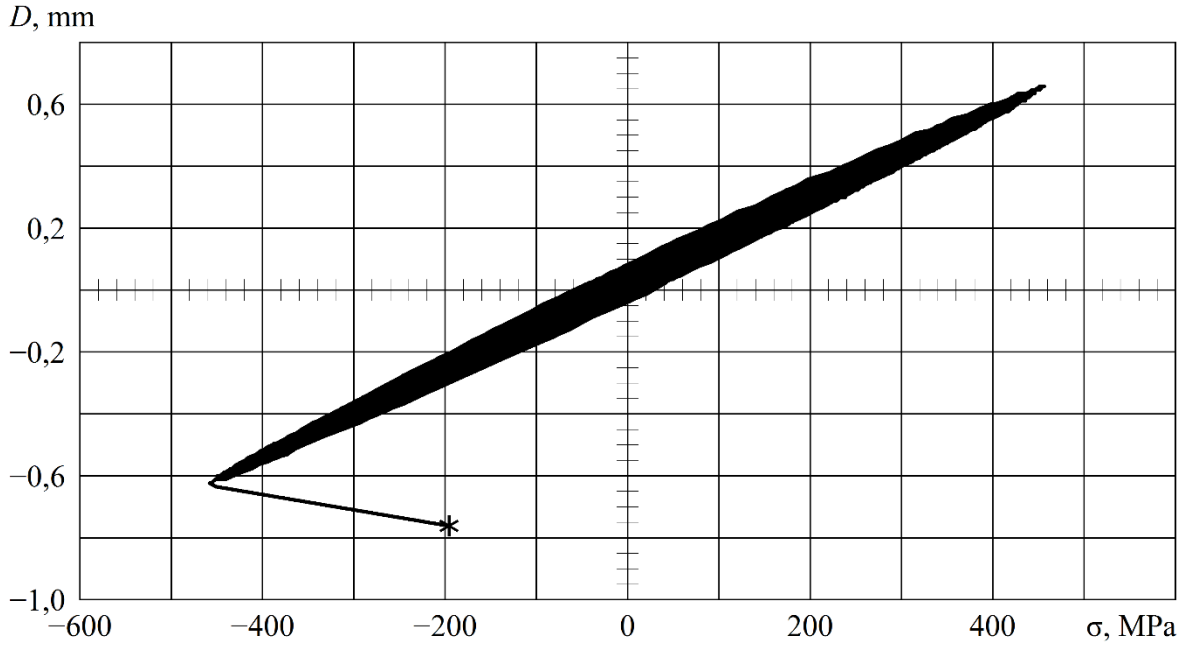

Figure 6. Inelastic behavior of a specimen cut from plate 1

To calculate the width of the loops, their median part in the stress range of ±0.5 of the amplitude was approximated by parabolas, according to which their width was calculated. For example, for the loading curve, the equation $D(\sigma)$ is obtained in the form

$$\delta D = y_2 - y_1 = (A_2 - A_1)x^2 + (B_2 - B_1)x + C_2 - C_1 = Ax^2 + Bx + C .$$

Taking the derivative and equating it to zero, we get the value σ, at which δD is the maximum ($\delta D = \Delta D$) — $x_* = \sigma_* = -B / 2A$, from where $\Delta D = Ax_*^2 + Bx_* + C$. The value $x_* = \sigma_*$ should not differ

significantly from the mean value $\sigma_m = (\sigma_{max} + \sigma_{min})/2$. In composites, with high absolute values of the asymmetry index $|a| = |\sigma_m|/\sigma_a$, the maximum width of the inelasticity loop is usually due to stresses $|\sigma| > |\sigma_m|$.

The amplitude dependence of the width of the inelasticity loops for the specimen from plate 1 is shown in Figure 7. The arrow marks the loading amplitude σ_{a0}, at which the first bend appears in the amplitude dependence of inelasticity, which means the appearance of local plastic strains in the structure of the material, most likely associated with the beginning of the composite stratification.

In the amplitude dependence of the width of the loops, several bends are observed, indicating the appearance of new places associated with the structure of the material in which plastic strains appear. To compare the inelastic characteristics of plate specimens with different exposure histories, we will compare the initial sections of the amplitude dependence of inelasticity and the width of loops at the same loading amplitudes. In addition, inelasticity at given amplitude can be divided into relaxation and hysteresis parts. The results of the inelastic behavior of the plate specimens are shown in Table 3.

For specimens of plates 1–3, this Table shows the average maximum stresses during fracture. The initial sections of the relaxation part of the inelasticity are represented by the amplitude σ_{a0}, after which the hysteresis component of inelasticity appears, and the intensity of the increase in inelasticity of the relaxation type (width of the loop) $|d\Delta D_r/d\sigma_a|$. The following column of Table 3 shows the values of the absorption coefficient ψ_r

$$\psi_r = \frac{\Delta W}{W} \approx \frac{\pi |d\,\Delta D_r / d\,\sigma_a|}{J} \qquad (6)$$

as the ratio of the energy absorbed in the cycle ΔW to the work of external forces W, expressed in terms of the intensity of the increase in relaxation type inelasticity with the pliability of specimens J (this is inverse of rigidity), calculated at σ_a = 50 MPa, that is, in the amplitude-independent region.

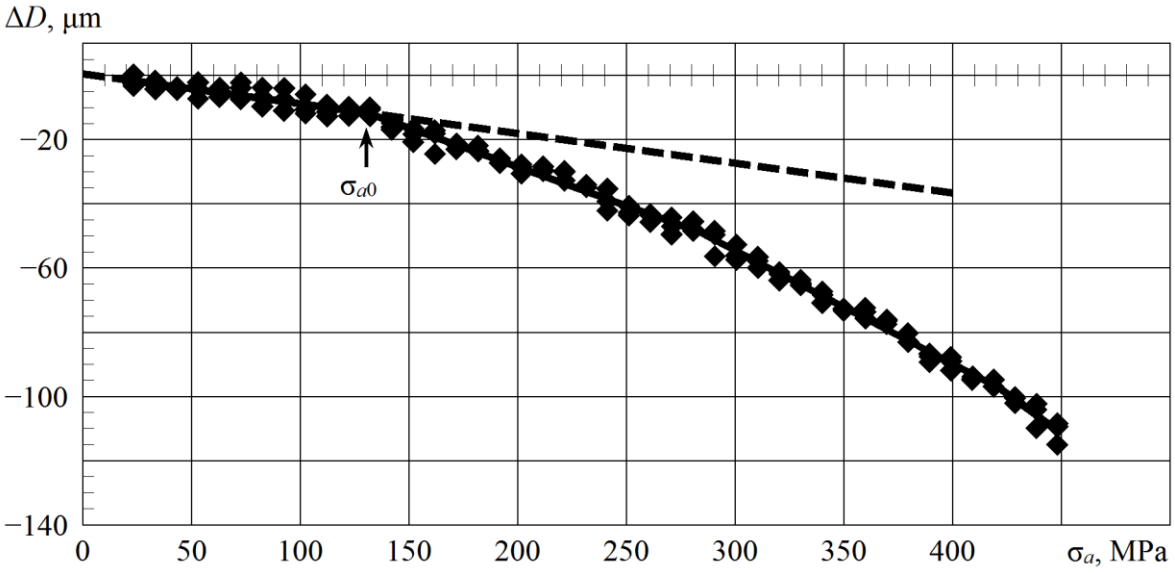

Figure 7. Amplitude dependence of the width of the inelasticity loops of the specimen from plate 1: σ_{a0} is amplitude of appearance of hysteresis type inelasticity

Table 3. Comparative characteristics of the average values of strength and inelasticity of specimens after climatic tests

Plate	$\|\sigma_{max}\|$, MPa	σ_{a0}, MPa	ψ_r	σ_a = 400 MPa		
				$\|\Delta D\|$, μm	$\|\Delta D_h\|$, μm	$\|\Delta D_h\|/\|\Delta D\|$
1	466	107	0.185	77.7	49.8	0.64
2	524	134	0.167	52.4	29.3	0.56
3	483	101	0.183	68.1	42.0	0.62

To compare the inelasticity of both types and their ratio, the contributions of relaxation and hysteresis energy losses at loading amplitude of 400 MPa were separated. To do this, the component of the width of the loops of the initial section of the amplitude dependence of the inelasticity (a straight line from the origin in Figure 7 to the

amplitude σ_{a0}), extrapolated to an amplitude of 400 MPa by a dashed line, was subtracted from the full width of the loops of inelasticity ΔD. The result is represented by the hysteresis fraction of the width of the loop $|\Delta D_h|$.

The results of cyclic tests presented in Table 3 confirm the increase in the strength of the plate 2 exposed under the canopy, noted in Table 2. After 7 years of being under a canopy, the σ_{max} increases by 13%. Table 3 also shows the average values of the calculated inelasticity characteristics for each type of plate, including the relative contribution of the hysteresis part of the inelasticity to its full value. It turned out that the characteristics of the inelasticity of the plate specimens, both in terms of relaxation and hysteresis energy absorption, fully correspond to their strength parameters.

The lowest strength of the specimens of plate 1 quite logically corresponds to the highest damping, both in absolute value and in the contribution of the hysteresis part of energy absorption. The best strength characteristics are possessed by the specimens of plate 2, and its damping properties are also the best, which is reflected in the best characteristics of the interlaminar shear (Table 2). The specimens of plate 3, both in strength and inelasticity, approach the characteristics of the initial state of the material, but still slightly surpassing them. Thus, solar radiation reduces the load-bearing capacity of the material obtained by it during prolonged exposure to protected conditions.

If the PCM is under the influence of direct solar radiation, then the processes of binder destruction are activated in the thin surface layer, forming a gradient of properties along the thickness of the plates [3]. Overheating of the surface contributes to the desorption of water molecules from the volume of the material [16] and a decrease in the plasticizing effect of moisture, thereby increasing the complex of deformation and strength parameters of the PCM [28].

There are repeatedly verified results, considered, for example, in works [29–31], which show the effect of structural relaxation on changes in mechanical parameters of PCM at the initial stages of thermal moisture [29] or climatic [30, 31] aging. If the epoxy matrix of the PCM is not fully cured [29, 30] or excessive internal stresses persist in it due to suboptimal cooling conditions of the pressed plates [31], then at the initial stages of aging, an increase in the strength and elastic parameters of the PCM is detected [30] or an abrupt change in elastic modulus due to relaxation of internal stresses [31].

To obtain information about the change in the molecular weight of the polymer matrix PCM during aging, the average molecular weight of the interstitial fragment of the spatial grid of the polymer matrix can be measured [32]. To do this, it is necessary to measure the elastic modulus E of the composite at the temperature of transition of the polymer to a highly elastic state. In that case, the value of E follows the mixture rule

$$E_1 = E_1 w + E_2 (1 - w),$$

where E_1 is the elastic modulus of the filler, $E_2 = 3F\rho RT(M_n)^{-1}$ is the elastic modulus of the polymer matrix, w is the degree of filling, M_n is the average molecular weight of the interstitial fragment of the spatial grid of the polymer matrix, ρ is the density of the polymer matrix, F is the front factor taking into account the deviation of the spatial grid from the ideal, R is the universal gas constant, T is the absolute temperature.

The decrease in M_n is a reliable indicator of the continuation of the curing process of the PCM polymer matrix. We expect to make such an assessment of M_n at the next stage of the work.

During the long-term stay of PCM in open climatic conditions, along with the control of a complex of strength indicators, it is necessary to control their deformation characteristics in the glassy and highly elastic states of the binder, the glass transition temperature of the polymer matrix, the coefficient of linear thermal expansion, moisture diffusion coefficients, moisture content and other physical indicators. This helps to understand the mechanism of aging of the PCM and determine the feasibility of using this material in the structural element of the product.

As for other climatic conditions, a systematic analysis of the influence of climate on the mechanical properties of PCM, carried out in [3], revealed the following pattern. If the material is resistant to thermal cycles and moisture in a warm, humid climate, then it will be even more resistant in a cold, moderately cold, dry climate.

A typical view of the failure specimens is shown in Figure 8. This type of fracture qualifies as creep failure. This is primarily due to the creep of the matrix in the composite, which contributes to the curvature of the fibers in it and their earlier fracture.

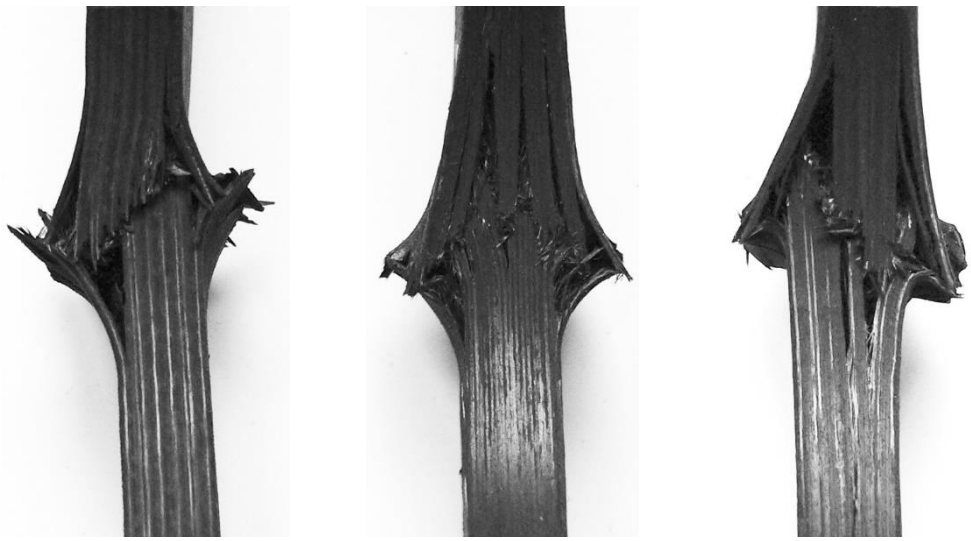

a *b* *c*

Figure 8. View of the fractures of the specimens cut from the plates 1 (*a*), 2 (*b*) and 3 (*c*)

Each of the specimens failed at that loading amplitude and at a time when damage from compressive loads led to the loss of its bearing capacity. All differences in their strength properties reflect the results of the thermal activation analysis shown in Figure 9. The value U_0 = 155.3 ± 8 kJ/mol is assumed to be the same as shown in Figure 4 for the interlaminar shear, and we connect it with the centers of scattering of the U_i values of individual specimens.

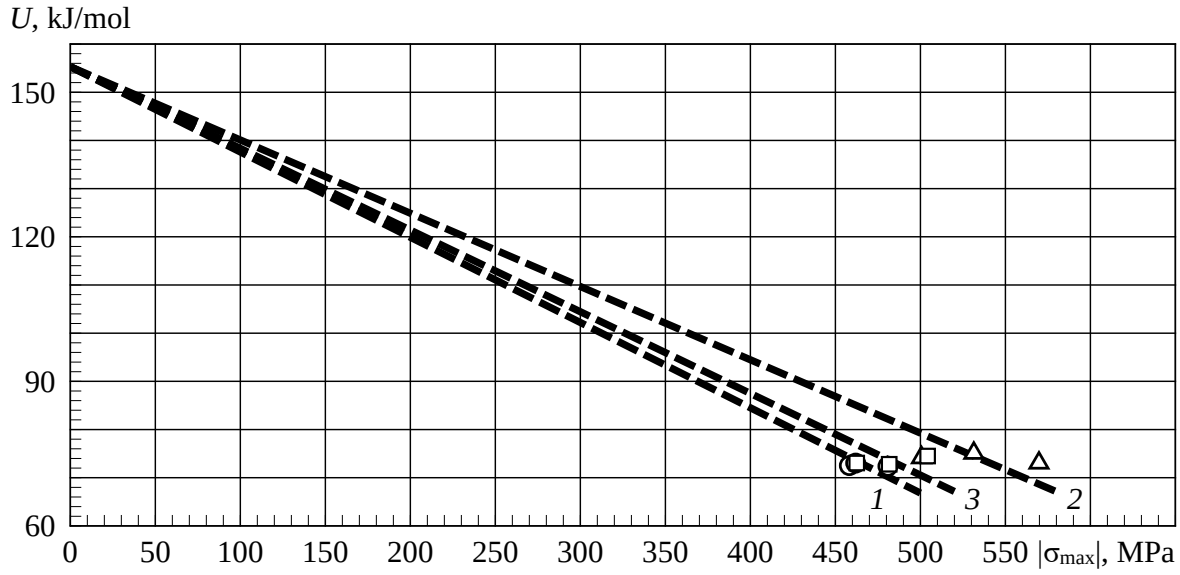

Figure 9. Force dependences of the FAE of specimens at initial state (*1*), after climatic test under a canopy (*2*), and on an open stand (*3*)

U_i values are calculated using a similar (2) expression (7)

$$\int_0^{t_*} \dot{\omega}(t,\sigma)dt = \tau_{eq}\nu_0 \exp\left(-\frac{U_0 - \gamma\,|\,\sigma_{\max}\,|}{RT}\right), \tag{7}$$

in which integration is also performed numerically in time steps. By presenting equation (3) for this case as

$$d\omega/dt = A\exp(B|\sigma|), \tag{8}$$

where $A = \nu_0 \exp[-U_0/(RT)]$ and $B = \gamma/(RT)$, we obtain for constant stresses the expression of damage ω in the form:

$$\omega = \omega_0 + A\exp(B\,|\,\sigma_0\,|)t\,.$$

For linearly increasing or linearly decreasing stresses, integration (8) gives

$$\omega = \omega_0 + A\exp(B\,|\,\sigma_0\,|)\frac{\exp(BVt)-1}{BV}.$$

In these expressions, ω_0 is the damage at the beginning of the time step t, $|\sigma_0|$ is the absolute value of the compression stresses at the beginning of the time step, V is the loading rate $d\sigma/dt$, substituted into the equation with the appropriate sign.

From equality (7), we determine the equivalent failure time corresponding to the maximum stress, and similarly (4) we obtain the force dependences of the FAE, according to which the durability of this carbon fiber can be recalculated for other temperature and force conditions, setting temperature, stresses and their rate of change at each time step. In this way, the problem of predicting the durability of a material under arbitrary changes in temperature and stress is solved. The failure time is a single characteristic of strength under all types of loading [26, 33].

In case of fatigue failure of materials, it is impossible to conduct a thermal activation analysis, since local failure processes are distributed over the volume of the material. In this case, it is necessary to proceed to the mathematical modeling of the set of processes distributed in the volume of the material [33]. In this paper, only the failure processes associated with the creep of the binder are considered. Only it makes it possible for the composite to withstand compression loads.

The results obtained show that the continuous presence of carbon fiber under the influence of climatic factors gives a different effect than moisture saturation–freezing, which simulates the real operating conditions of aircraft structures and reduces its strength characteristics [12, 18]. But in both cases, the approach used based on the kinetic concept of fracture, considering the failure process as a set of internal thermodynamic processes, provides new information about the properties of the material [33]. This makes it possible to predict the durability of various materials under arbitrary temperature-force and temperature-time conditions.

5. Conclusions

CFRP based on Cycom 977-2 epoxy binder and Tenax ® IMS carbon fiber, after 7 years of exposure to a warm, humid climate, exhibits high resistance to variable temperature and humidity conditions. After exposure under a canopy, strength indicators increase both with interlayer shear and with cyclic tension–compression by 7–13%. This characterizes this binder composition, the properties of which are favorably influenced by prolonged thermal exposure at varying temperatures. As a result of such a "technological operation", the bearing capacity of the composite increases under compressive loads that is the most important thing.

If the surface of carbon fiber is under the direct influence of solar radiation, then the strength characteristics of the material decrease slightly, but remain at the level of initial values. This requires the protection of this material from the effects of solar radiation (reflective or absorbing coatings).

The conducted research shows the advantage of using the kinetic concept of fracture for PCM to interpret the failure processes as thermodynamic caused by thermal activation. This approach is the basis for predicting the durability of materials under variable temperature and force conditions. The values of temperature, stress, and activation volume characterizing the change in the structure of the material may differ at each time step of the calculations. In this way, the problem of durability prediction with arbitrary changes in temperature and stresses is solved.

Acknowledgments

The authors express their appreciation for the valuable suggestions of the reviewers and a very useful discussion that made it possible to improve the content of the article.

Conflict of interest

The authors declare no conflict of interest.

References

[1] Baker DJ. Ten-Year Ground Exposure of Composite Materials Used on the Bell Model 206L Helicopter Flight Service Program. Hampton. Virginia: NASA Technical Paper 3468, ARL Technical Report 480; 1994.
[2] Kablov EN (ed.). Aviation materials. Handbook in 13 volumes. Vol. 13. Climatic and microbiological resistance of non-metallic materials. Moscow: All-Russian Research Institute Aviation Materials (VIAM); 2015. [in Russian]
[3] Kablov, E.; Federal state unitary enterprise «All-Russian scientific research institute of aviation materials»; Startsev, V. SYSTEMATICAL ANALYSIS OF THE CLIMATICS INFLUENCE ON MECHANICAL PROPERTIES OF THE POLYMER COMPOSITE MATERIALS BASED ON DOMESTIC AND FOREIGN SOURCES (review). *«Aviation Mater. Technol.* **2018**, https://doi.org/10.18577/2071-9140-2018-0-2-47-58.
[4] Vapirov YuM. Mechanisms of aging of carbon fiber plastics for aviation purposes in a warm humid climate. Dissertation of the Candidate of Technical Sciences. Moscow: VIAM; 1989. [In Russian]
[5] Vapirov YuM, Krivonos VV, Startsev OV. Interpretation of the anomalous change in the properties of carbon-fiber-reinforced plastic KMU-1U during aging in different climatic regions . Mechanics of Composite Materials. 1994; 30: 190–194.
[6] Dexter HB. Long-term environmental effects and flight service evaluation of composite materials. Report NASA: No. NASA TM-89067; 1987.
[7] Kudo A, Ben G. Estimation of weather ability flexural properties for CFRP subjected to long-term outdoor exposure. 18th International Conference on Composite Materials, 21–26 August 2011, Jeju Island, S. Korea. International Committee on Composite Materials: The Korean Society for Composite Materials; 2011. W27-3-IF1485.
[8] Vodicka R, Nelson B, van den Berg J, Chester R. Long-term environmental durability of F/A-18 composite material. DSTO-TN-0826. Melbourne, Australia: DSTO Aeronautical and Maritime Research Lab.; 1999.
[9] Gulyaev IN, Zelenina IV, Valyavin EO, Haskov MA. The influence of climatic aging on the properties of high-temperature carbon fiber plastics. Trudy VIAM. 2021; 2(96): 39–51. [In Russian]
[10] Koval TV, Vilegodsky IM, Gromova AM. Investigation of the plasticizing effect of moisture on the properties of PCM based on the epoxy binder VSE-34 after 5 years of exposure in various climatic zones. Trudy VIAM. 2021. 9(103): 105–116. [In Russian]
[11] Evdokimov AA, Petrova AP, Pavlovsky KA, Gulyaev IN. The effect of climatic aging on the properties of PCM based on an epoxy vinyl ester binder. Trudy VIAM. 2021. 3(97): 128–136. [In Russian]
[12] Lebedev, M.P.; Startsev, O.V.; Kychkin, A.K.; Petrov, M.G.; Kopyrin, M.M. Contributing Factors of Uneven Climatic Aging for Polymeric Composite Materials: Methods and Modelling. *Polymers* **2023**, *15*, 1458, https://doi.org/10.3390/polym15061458.
[13] Jumahat, A.; Soutis, C.; Jones, F.R.; Hodzic, A. Fracture mechanisms and failure analysis of carbon fibre/toughened epoxy composites subjected to compressive loading. *Compos. Struct.* **2010**, *92*, 295–305, https://doi.org/10.1016/j.compstruct.2009.08.010.
[14] Koushyar, H.; Alavi-Soltani, S.; Minaie, B.; Violette, M. Effects of variation in autoclave pressure, temperature, and vacuum-application time on porosity and mechanical properties of a carbon fiber/epoxy composite. *J. Compos. Mater.* **2011**, *46*, 1985–2004, https://doi.org/10.1177/0021998311429618.
[15] Kolesnik KA. Modeling of moisture saturation of polymer composites in real climatic conditions. Aviation materials and technologies. 2017; (4): 77–86. [In Russian]
[16] Salnikov VG, Startsev OV, Lebedev MP, Kopyrin MM, Vapirov YuM. The influence of daily and seasonal changes in relative humidity and temperature on moisture saturation of carbon fiber in open climatic conditions. Vse materialy. Entsiklopedicheskiy spravochnik (All materials. Encyclopedic reference book). 2022; (5): 2–10. [In Russian]
[17] Lebedev, M.P.; Startsev, O.V.; Petrov, M.G.; Kopyrin, M.M. The Formation of Microcracks during Climatic Aging of Polymer-Composite Materials. *Polym. Sci. Ser. D* **2023**, *16*, 116–123, https://doi.org/10.1134/s199542122301015x.
[18] Petrov, M.G.; Lebedev, M.P.; Startsev, O.V.; Kopyrin, M.M. Effect of Low Temperatures and Moisture on the Strength Performance of Carbon Fiber Reinforced Plastic. *Dokl. Phys. Chem.* **2021**, *500*, 85–91, https://doi.org/10.1134/s0012501621090037.
[19] Asasaari S.F.M., Wong K.J., Tamin M.N. Moisture absorption effects on the mechanical properties of carbon/epoxy composites. International Journal of Structural Integrity. 2020; 11: 605–614.
[20] Cruz, R.; Correia, L.; Dushimimana, A.; Cabral-Fonseca, S.; Sena-Cruz, J. Durability of Epoxy Adhesives and Carbon Fibre Reinforced Polymer Laminates Used in Strengthening Systems: Accelerated Ageing versus Natural Ageing. *Materials* **2021**, *14*, 1533, https://doi.org/10.3390/ma14061533.

[21] Robin, A.; Arhant, M.; Davies, P.; Lejeune, S.; Lolive, E.; Bonnemains, T.; Habert, B. Effect of aging on the in-plane and out-of-plane mechanical properties of composites for design of marine structures. *Compos. Part C: Open Access* **2023**, *11*, https://doi.org/10.1016/j.jcomc.2023.100354.
[22] Shi Z., Zou C., Zhou F., Zhao J. Analysis of the mechanicalproperties and damage mechanism of carbon fiber/epoxy composites under UV aging. Materials. 2022; 15: Article 2919.
[23] Gillespie Jr. JW, Carlsson LA, Smiley AJ. Rate-dependent mode I interlaminar crack growth mechanisms in graphite/epoxy and graphite/PEEK. Composites Science and Technology. 1987; 28: 1–15.
[24] Suvorova, Y.V.; Sorina, T.G.; Gunyaev, G.M. Rate dependences of the strength of carbon-fiber-reinforced plastics. *Mech. Compos. Mater.* **1991**, *26*, 480–484, https://doi.org/10.1007/bf00612621.
[25] Merkulov SI, Esipov SM. The influence of the rate and loading mode on the strength and rigidity of reinforced carbon fiber plastics. Bulletin of BSTU named after VG Shukhov. 2017; (1): 52–56. [In Russian]
[26] Regel BP, Slutsker AI, Tomashevsky EE. The kinetic nature of the strength of solids. Moscow: "Nauka"; 1974. [In Russian]
[27] Nikolaev EV, Pavlov MR, Andreeva NP, Slavin AV, Skirta AA. Investigation of the aging processes of polymer composite materials in natural conditions of the tropical climate of North America. News of Materials Science. Science and technology. 2018; (3–4): 61–70. [In Russian]
[28] Startsev VO, Slavin AV. Resistance of carbon fiber and fiberglass based on molten binders to the effects of moderately cold and moderately warm climates. Trudy VIAM. 2021; 5(99): 114–126. [In Russian]
[29] Startsev, O.V.; Anikhovskaya, L.I.; Litvinov, A.A.; Krotov, A.S. Increasing the reliability of predicting the properties of polymer composites in hygrothermal aging. *Dokl. Chem.* **2009**, *428*, 228–232, https://doi.org/10.1134/s0012500809090079.
[30] Startseva, L.T. Climatic aging of organic-fiber-reinforced plastics. *Mech. Compos. Mater.* **1994**, *29*, 620–626, https://doi.org/10.1007/bf00616330.
[31] Kablov, E.N.; Startsev, V.O. The Influence of Internal Stresses on the Aging of Polymer Composite Materials: a Review. *Mech. Compos. Mater.* **2021**, *57*, 565–576, https://doi.org/10.1007/s11029-021-09979-6.
[32] Startsev VO, Vardanyan AM. Influence of external influences on the coefficient of linear thermal expansion of carbon fiber plastics. Part 1. Analysis of theoretical and experimental results (review). Trudy VIAM. 2023; 2(120): 147–168. Available at: http://www.viam-works.ru. DOI: 10.18577/2307-6046-2023-0-2-147-168. [In Russian]
[33] Petrov, M. Fracturing of Solids as a Thermodynamic Process. *Alloys* **2023**, *2*, 122–139, https://doi.org/10.3390/alloys2030009.